 SL, vol.6, no.2, pp.93-107, 2011

Compact Local Stencils Employed With Integrated RBFs For Fourth-Order Differential Problems

T.-T. Hoang-Trieu[1], **N. Mai-Duy**[1] **and T. Tran-Cong**[1]

Abstract: In this paper, new compact local stencils based on integrated radial basis functions (IRBFs) for solving fourth-order ordinary differential equations (ODEs) and partial differential equations (PDEs) are presented. The integration constants arising from the construction of IRBFs are exploited to incorporate into the local IRBF approximations values of the ODEs/PDEs at selected nodal points. The proposed stencils, which lead to sparse system matrices, are numerically validated through the solution of several analytic test problems. Numerical results indicate that their solutions converge very fast with grid refinement.

Keywords: Compact local approximations, high-order ODEs, high-order PDEs, integrated radial basis functions.

1 Introduction

Numerical techniques have been developed to solve ODEs and PDEs which are used to model continuum mechanics problems such as the motion of a fluid and the deformation of a solid body. Traditional discretisation methods include finite-difference methods (FDMs), finite-element methods (FEMs) and boundary-element methods (BEMs). Over the last 20 years, RBFs, which are known as a universal approximator, have been applied for the solution of ODEs and PDEs. They were first developed as a global technique, in which the dependent variable is decomposed into a set of RBFs defined over the whole domain, and its derivatives are then calculated through differentiation (differentiated RBFs (DRBFs)) [Kansa (1990b)]. Later on, Mai-Duy and Tran-Cong (2001) proposed integrated RBF (IRBF) methods, in which highest-order derivative(s) in the ODE/PDE are approximated by RBFs, and lower-order derivatives and the dependent variable itself are then obtained by integration. Numerical results showed that IRBFs yield better accuracy than DRBFs.

[1] Computational Engineering and Science Research Centre, Faculty of Engineering and Surveying, University of Southern Queensland, Toowoomba, QLD 4350, Australia.

Global IRBF methods have some strengths and weaknesses. They can produce very accurate solutions using relatively low numbers of data nodes, and their implementations are quite straightforward. However, they lead to fully populated system matrices. As a result, for a given spatial discretisation, larger requirements for computer's storage are needed when compared with traditional methods. In addition, the condition number of the global IRBF matrices grows very quickly as the number of nodes increases. To overcome these drawbacks, local and compact local IRBF schemes have been developed (e.g. [Mai-Duy and Tran-Cong (2009), Ngo-Cong, Mai-Duy, Karunasena, and Tran-Cong (2010), An-Vo, Mai-Duy, and Tran-Cong (2011), Mai-Duy and Tran-Cong (2011)]). The obtained system matrices are sparse and their solutions are thus more efficient. In Mai-Duy and Tran-Cong (2011), compact local IRBF stencils for solving Poisson equation on rectangular and non-rectangular domains were proposed; compact local forms are able to produce much more accurate results than local forms.

This paper is concerned with the development of compact local IRBF stencils for the solution of fourth-order ODEs and PDEs. We will present a 5-node stencil for 1D problems and a 5×5-node stencil for 2D problems. The remainder of the paper is organised as follows. Section 2 is a brief review of IRBFs. The proposed compact local stencils based on IRBFs for 1D and 2D problems are presented in Section 3. Numerical examples are given in Section 4. Section 5 concludes the paper.

2 Brief review of integrated RBFs

Consider a fourth-order DE. In the IRBF methods, the highest-order derivatives (i.e. fourth-order ones under consideration here) of the field variable u are decomposed into a set of RBFs:

$$\frac{\partial^4 u(\eta)}{\partial \eta^4} = \sum_{i=1}^{n} w_i I_i^{(4)}(\eta) \tag{1}$$

where η denotes a component of the position vector $\mathbf{x}$ (e.g. η can be x for 1D problems, and x or y for 2D problems), $\{w_i\}_{i=1}^n$ is the set of RBF coefficients, and $\left\{I_i^{(4)}(\mathbf{x})\right\}_{i=1}^n$ is the set of RBFs. Expressions (1) is then integrated to obtain approximations to lower order derivatives and the function:

$$\frac{\partial^3 u(\eta)}{\partial \eta^3} = \sum_{i=1}^{n} w_i I_i^{(3)}(\eta) + c_1 \tag{2}$$

$$\frac{\partial^2 u(\eta)}{\partial \eta^2} = \sum_{i=1}^{n} w_i I_i^{(2)}(\eta) + \eta c_1 + c_2 \tag{3}$$

$$\frac{\partial u(\eta)}{\partial \eta} = \sum_{i=1}^{n} w_i I_i^{(1)}(\eta) + \frac{\eta^2}{2} c_1 + \eta c_2 + c_3 \tag{4}$$

$$u(\eta) = \sum_{i=1}^{n} w_i I_i^{(0)}(\eta) + \frac{\eta^3}{6} c_1 + \frac{\eta^2}{2} c_2 + \eta c_3 + c_4 \tag{5}$$

where c_1, c_2, c_3 and c_4 are "constant of integration" with respect to η, which are to be treated as the additional RBF coefficients. In (1) - (5), the superscript (.) is used to indicate the associated derivative order. In this study, the multiquadric (MQ) function is chosen as the basis function:

$$I_i^{(4)}(x) = \sqrt{(x - c_i)^2 + a_i^2} \quad \text{for 1D problems} \tag{6}$$

$$I_i^{(4)}(\mathbf{x}) = \sqrt{(x - c_{ix})^2 + (y - c_{iy})^2 + a_i^2} \quad \text{for 2D problems} \tag{7}$$

where c_i (for 1D problems) or $(c_{ix}, c_{iy})^T$ (for 2D problems) and a_i are the MQ centre and width, respectively. The width of the ith MQ can be determined according to the following relation:

$$a_i = \beta d_i \tag{8}$$

where β is a factor (β>0) and d_i is the distance from the ith centre to the nearest neighbour. It was observed in [Kansa (1990a)] that, as the RBF width increases, the numerical error of the RBF solution reduces and the condition number of the interpolant grows. At large values of β, one needs to pay special attention as the solution becomes unstable. Values of β were reported to be 1 for global IRBF methods and in a wide range of $2-200$ for local and compact local IRBF methods. For the latter, one can vary the value of β and/or refine the spatial discretisation to enhance the solution accuracy.

3 Proposed compact local IRBF stencils for fourth-order ODEs and PDEs

3.1 Compact local 5-node stencil for ODEs

Our sample of fourth-order ODEs is taken as

$$\frac{d^4 u}{dx^4} + \frac{d^2 u}{dx^2} = f(x) \tag{9}$$

where $x_A \leq x \leq x_B$ and $f(x)$ is some given function. The boundary conditions prescribed here are of Dirichlet type, i.e. u and du/dx given at x_A and x_B.

We discretise the problem domain using a set of n discrete nodes. Consider a grid node x_i with $i = \{3,4,\cdots,n-2\}$ and its associated 5-node stencil $[x_1^i, x_2^i, x_3^i, x_4^i, x_5^i]$ ($x_i \equiv x_3^i$).

The conversion system, which represents the relation between the RBF space and the physical space, is established from the following equations

$$\begin{pmatrix} \widehat{u} \\ \widehat{e} \end{pmatrix} = \underbrace{\begin{bmatrix} \mathscr{H}^{(0)} \\ \mathscr{K} \end{bmatrix}}_{\mathscr{C}} \begin{pmatrix} \widehat{w} \\ \widehat{c} \end{pmatrix} \tag{10}$$

where $\mathscr{C}$ is the conversion matrix, $\widehat{u} = \mathscr{H}^{(0)}\,(\widehat{w},\widehat{c})^T$ are equations representing nodal values of u over the stencil, $\widehat{u} = (u_1,u_2,u_3,u_4,u_5)^T$, $\widehat{w} = (w_1,w_2,w_3,w_4,w_5)^T$, $\widehat{c} = (c_1,c_2,c_3,c_4)^T$, $\mathscr{H}^{(0)}$ is a 5×9 matrix that is obtained from collocating (5) at grid nodes of the stencil

$$\mathscr{H}^{(0)} = \begin{bmatrix} I_1^{(0)}(x_1^i), & \ldots, & I_5^{(0)}(x_1^i), & (x_1^i)^3/6, & (x_1^i)^2/2, & x_1^i, & 1 \\ I_1^{(0)}(x_2^i), & \ldots, & I_5^{(0)}(x_2^i), & (x_2^i)^3/6, & (x_2^i)^2/2, & x_2^i, & 1 \\ I_1^{(0)}(x_3^i), & \ldots, & I_5^{(0)}(x_3^i), & (x_3^i)^3/6, & (x_3^i)^2/2, & x_3^i, & 1 \\ I_1^{(0)}(x_4^i), & \ldots, & I_5^{(0)}(x_4^i), & (x_4^i)^3/6, & (x_4^i)^2/2, & x_4^i, & 1 \\ I_1^{(0)}(x_5^i), & \ldots, & I_5^{(0)}(x_5^i), & (x_5^i)^3/6, & (x_5^i)^2/2, & x_5^i, & 1 \end{bmatrix}$$

$\widehat{e} = \mathscr{K}\,(\widehat{w},\widehat{c})^T$ are equations representing extra information that can be the ODE (9) at selected nodes, and du/dx at x_A and x_B. Solving (10) results in

$$\begin{pmatrix} \widehat{w} \\ \widehat{c} \end{pmatrix} = \mathscr{C}^{-1} \begin{pmatrix} \widehat{u} \\ \widehat{e} \end{pmatrix} \tag{11}$$

If the number of extra information values are less than or equal to 4, the obtained conversion matrix in (10) is not overdetermined owing to the presence of the integration constants. In this case, the extra information is thus imposed in an exact manner.

By substituting (11) into (1)-(5), values of u and its derivatives at an arbitrary point

x on the stencil are calculated in the physical space as

$$\frac{d^4u(x)}{x^4} = \left[\begin{array}{cccccccc} I_1^{(4)}(x), & \ldots, & I_5^{(4)}(x), & 0, & 0, & 0, & 0 \end{array} \right] \mathscr{C}^{-1} \left(\begin{array}{c} \widehat{u} \\ \widehat{e} \end{array} \right) \tag{12}$$

$$\frac{d^3u(x)}{dx^3} = \left[\begin{array}{cccccccc} I_1^{(3)}(x), & \ldots, & I_5^{(3)}(x), & 1, & 0, & 0, & 0 \end{array} \right] \mathscr{C}^{-1} \left(\begin{array}{c} \widehat{u} \\ \widehat{e} \end{array} \right) \tag{13}$$

$$\frac{d^2u(x)}{dx^2} = \left[\begin{array}{cccccccc} I_1^{(2)}(x), & \ldots, & I_5^{(2)}(x), & x, & 1, & 0, & 0 \end{array} \right] \mathscr{C}^{-1} \left(\begin{array}{c} \widehat{u} \\ \widehat{e} \end{array} \right) \tag{14}$$

$$\frac{du(x)}{dx} = \left[\begin{array}{cccccccc} I_1^{(1)}(x), & \ldots, & I_5^{(1)}(x), & x^2/2, & x, & 1, & 0 \end{array} \right] \mathscr{C}^{-1} \left(\begin{array}{c} \widehat{u} \\ \widehat{e} \end{array} \right) \tag{15}$$

$$u(x) = \left[\begin{array}{cccccccc} I_1^{(0)}(x), & \ldots, & I_5^{(0)}(x), & x^3/6, & x^2/2, & x, & 1 \end{array} \right] \mathscr{C}^{-1} \left(\begin{array}{c} \widehat{u} \\ \widehat{e} \end{array} \right) \tag{16}$$

where $x_1^i \leq x \leq x_5^i$.

In the following, two approaches for the construction of the final system of algebraic equations, namely Implementation 1 and Implementation 2, are proposed. For each approach, we employ $\widehat{e} = \mathscr{K}\,(\widehat{w},\widehat{c})^T$ to represent values of (9) at x_2^i and x_4^i, i.e.

$$\left(\begin{array}{c} f\left(x_2^i\right) \\ f\left(x_4^i\right) \end{array} \right) = \left[\begin{array}{cccccccc} G_1(x_2^i), & \ldots, & G_5(x_2^i), & x_2^i, & 1, & 0, & 0 \\ G_1(x_4^i), & \ldots, & G_5(x_4^i), & x_4^i, & 1, & 0, & 0 \end{array} \right] \left(\begin{array}{c} \widehat{w} \\ \widehat{c} \end{array} \right)$$

where $i = \{3,4,\cdots,n-2\}$ for Implementation 1, $i = \{4,5,\cdots,n-3\}$ for Implementation 2 and $G_j(x_k^i) = I_j^{(4)}\left(x_k^i\right) + I_j^{(2)}\left(x_k^i\right)$, $k = \{2,4\}$.

Implementation 1: The final system is generated by the collocation of the ODE (9) at $\{x_3,x_4,\cdots,x_{n-2}\}$ using (12) and (14) with $x = x_i$, and the imposition of du/dx at x_A and x_B using (15) with $x = x_1$ and $x = x_n$.

Implementation 2: The final system is generated by collocating the ODE (9) at $\{x_4,x_5,\cdots,x_{n-3}\}$ and $\{x_2,x_3,x_{n-2},x_{n-1}\}$. For the former, the collocation process is similar to that of Implementation 1. For the latter, special treatments for the imposition of first derivative boundary conditions are required. Collocations of the ODE (9) at $\{x_2,x_3\}$ and $\{x_{n-2},x_{n-1}\}$ are based on the stencils of nodes x_3 and x_{n-2}, respectively, with the following modified extra information vector

$\widehat{e} = (du(x_1^i)/dx, f(x_4^i))^T$ for the stencil of x_3

$\widehat{e} = (f(x_2^i), du(x_5^i)/dx)^T$ for the stencil of x_{n-2}

Both implementations lead to a system matrix of dimensions $(n-2)\times(n-2)$.

3.2 Compact local 5×5-node stencil for PDEs

Consider a 2D fourth-order problem governed by the biharmonic equation

$$\frac{\partial^4 u}{\partial x^4} + 2\frac{\partial^4 u}{\partial x^2 y^2} + \frac{\partial^4 u}{\partial y^4} = f(x,y) \tag{17}$$

on a rectangular domain ($x_A \le x \le x_B$, $y_C \le y \le y_D$), and subject to Dirichlet boundary conditions (u and $\partial u/\partial n$ given at the boundaries (n the normal direction)).

The problem domain is replaced by a Cartesian grid $n_x \times n_y$, which is shown in Fig. 1.

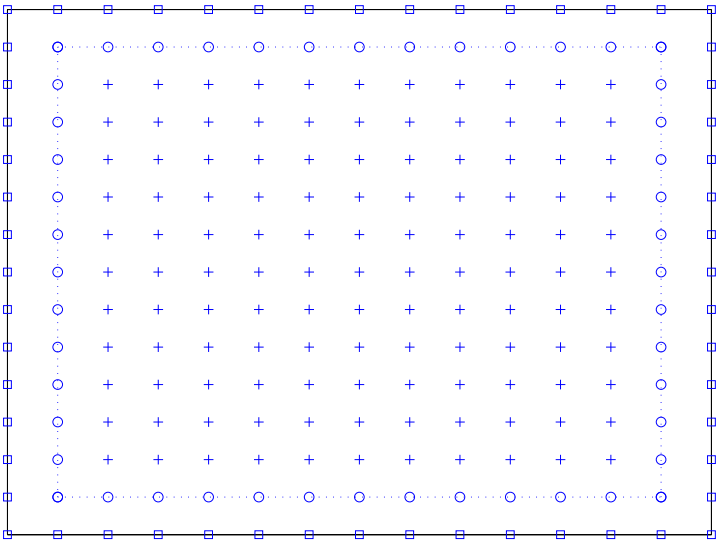

Figure 1: A problem domain and a typical discretisation. Legends square, circle and plus are used to denote the boundary nodes, the interior nodes next the boundary and the remaining interior nodes, respectively.

Consider a grid node (i,j) with ($3 \le i \le n_x - 2$ and $3 \le j \le n_y - 2$) and its associated 5×5-node stencil. The stencil is locally numbered from left to right and from bottom to top (node $(i,j) \equiv$ node 13) (Fig. 2). The solution procedure here is similar to that for 1D problems. However, the 2D problem formulation involves more terms and requires special treatments for interior "corner" nodes.

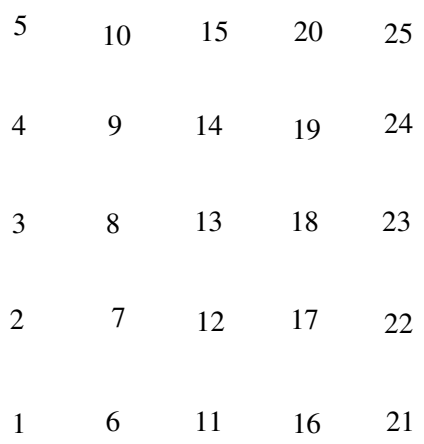

Figure 2: A 5×5-node stencil

The conversion system is constructed as

$$\begin{pmatrix} \widehat{u} \\ \widehat{0} \\ \widehat{e} \end{pmatrix} = \underbrace{\begin{bmatrix} \mathscr{H}_x^{(0)}, & \mathscr{O} \\ \mathscr{H}_x^{(0)}, & -\mathscr{H}_y^{(0)} \\ \mathscr{K}_x, & \mathscr{K}_y \end{bmatrix}}_{\mathscr{C}} \begin{pmatrix} \widehat{w}_x \\ \widehat{w}_y \end{pmatrix} \tag{18}$$

where the subscripts x and y denote the quantity associated with the integration process in the x and y direction, respectively, equations $\mathscr{H}_x^{(0)}\widehat{w}_x = \widehat{u}$ are employed to collocate the variable u over the stencil, equations $\mathscr{H}_x^{(0)}\widehat{w}_x - \mathscr{H}_y^{(0)}\widehat{w}_y = \widehat{0}$ are employed to enforce nodal values of u obtained from the integration with respect to x and y to be identical, and equations $\mathscr{K}_x\widehat{w}_x + \mathscr{K}_y\widehat{w}_y = \widehat{e}$ are employed to represent extra information that can be values of the PDE (9) at selected nodes on the stencil and first-order derivative boundary conditions. In (18), $\mathscr{C}$ is the conversion matrix, $\widehat{0}$ and $\mathscr{O}$ are a vector and a matrix of zeros, respectively, $\widehat{u}$ and $\widehat{0}$ are vectors of length 25; $(\widehat{w}_x, \widehat{w}_y)^T$ is the RBF coefficient vector of length 90, and $\mathscr{O}, \mathscr{H}_x^{(0)}, \mathscr{H}_y^{(0)}, \mathscr{K}_x$ and $\mathscr{K}_y$ are matrices (the first three are of dimensions 25×45, while for the last two, their dimensions are dependent on the number of extra information values imposed and typically vary between 4×45 and 8×45). Solving (18) yields

$$\begin{pmatrix} \widehat{w}_x \\ \widehat{w}_y \end{pmatrix} = \mathscr{C}^{-1} \begin{pmatrix} \widehat{u} \\ \widehat{0} \\ \widehat{e} \end{pmatrix} \tag{19}$$

We also propose two approaches, namely Implementation 1 and Implementation 2, to form the final set of algebraic equations.

Implementation 1: The final system is composed of two sets of equations. The first set is obtained by collocating the PDE and the second set is obtained by imposing first derivative boundary conditions.

Implementation 2: First derivative boundary conditions are incorporated into the conversion system and the final system is formed by collocating the PDE only.

Some implementation notes:

1. In constructing the approximations for stencils, the cross derivative $\partial^4 u/\partial x^2 \partial y^2$ is computed through the following relation [Mai-Duy and Tanner (2005)], which requires the approximation of second-order pure derivatives only,

$$\begin{aligned}\frac{\partial^4 u}{\partial^2 x \partial^2 y} &= \frac{1}{2}\left(\frac{\partial^2}{\partial x^2}\left(\frac{\partial^2 u}{\partial y^2}\right)+\frac{\partial^2}{\partial y^2}\left(\frac{\partial^2 u}{\partial x^2}\right)\right)\\ &= \frac{1}{2}\left(\mathscr{H}_x^{(2)}\left[\mathscr{H}_x^{(0)}\right]^{-1}\left(\mathscr{H}_y^{(2)}\widehat{w}_y\right)+\mathscr{H}_y^{(2)}\left[\mathscr{H}_y^{(0)}\right]^{-1}\left(\mathscr{H}_x^{(2)}\widehat{w}_x\right)\right)\end{aligned} \tag{20}$$

2. In constructing $\widehat{e} = \mathscr{K}_x\widehat{w}_x + \mathscr{K}_y\widehat{w}_y$, we choose four nodes placed in the diamond in Fig. 2 (i.e $(i-1,j),(i,j-1),(i,j+1)$ and $(i+1,j)$) to collocate the PDE (17). $\mathscr{K}_x$ and $\mathscr{K}_y$ can thus be expressed in the form

$$\mathscr{K}_x = \mathscr{H}_x^{(4)}(\mathbf{x}_\diamond) + \mathscr{H}_y^{(2)}(\mathbf{x}_\diamond)\left[\mathscr{H}_y^{(0)}\right]^{-1}\mathscr{H}_x^{(2)}$$

$$\mathscr{K}_y = \mathscr{H}_y^{(4)}(\mathbf{x}_\diamond) + \mathscr{H}_x^{(2)}(\mathbf{x}_\diamond)\left[\mathscr{H}_x^{(0)}\right]^{-1}\mathscr{H}_y^{(2)}$$

where $x_\diamond$ represents the coordinates of the four points $\{8,12,14,18\}$.

3. The collocations of (17) at four interior "corner" nodes (i.e. $(2,2)$, $(2,n_y-1)$, $(n_x-1,2)$ and (n_x-1,n_y-1)) are based on the stencils of four nodes $(3,3),(3,ny-2),(nx-2,3)$ and $(nx-2,ny-2)$ with the modified extra information vectors. For example, in the case of $(2,2)$, we modify $\widehat{e} = \mathscr{K}_x\widehat{w}_x + \mathscr{K}_y\widehat{w}_y$ as

$$\begin{pmatrix} \dfrac{\partial u(\mathbf{x}_2)}{\partial x} \\ \dfrac{\partial u(\mathbf{x}_3)}{\partial x} \\ \dfrac{\partial u(\mathbf{x}_6)}{\partial y} \\ \dfrac{\partial u(\mathbf{x}_{11})}{\partial y} \\ f(\mathbf{x}_{14}) \\ f(\mathbf{x}_{18}) \end{pmatrix} = \begin{bmatrix} \mathscr{H}_x^{(1)}(\mathbf{x}_2), & \mathscr{O} \\ \mathscr{H}_x^{(1)}(\mathbf{x}_3), & \mathscr{O} \\ \mathscr{O}, & \mathscr{H}_y^{(1)}(\mathbf{x}_6) \\ \mathscr{O}, & \mathscr{H}_y^{(1)}(\mathbf{x}_{11}) \\ G_{[x]}(\mathbf{x}_{14}), & G_{[y]}(\mathbf{x}_{14}) \\ G_{[x]}(\mathbf{x}_{18}), & G_{[y]}(\mathbf{x}_{18}) \end{bmatrix} \begin{pmatrix} \widehat{w}_x \\ \widehat{w}_y \end{pmatrix} \tag{21}$$

where $\mathbf{x} = (x, y)^T$,
$G_{[x]}(\mathbf{x}_k) = \mathscr{H}_x^{(4)}(\mathbf{x}_k) + \mathscr{H}_y^{(2)}(\mathbf{x}_k)\left[\mathscr{H}_y^{(0)}\right]^{-1}\mathscr{H}_x^{(2)}$,
and
$G_{[y]}(\mathbf{x}_k) = \mathscr{H}_y^{(4)}(\mathbf{x}_k) + \mathscr{H}_x^{(2)}(\mathbf{x}_k)\left[\mathscr{H}_x^{(0)}\right]^{-1}\mathscr{H}_y^{(2)}$, k=$\{14, 18\}$
Both Implementation 1 and Implementation 2 lead to a final system matrix of dimensions $(n_x-2)(n_y-2)\times(n_x-2)(n_y-2)$.

4 Numerical examples

We measure the accuracy of an approximation scheme in the form

$$Ne(u) = \frac{\sqrt{\sum_{i=1}^{n}(u_i - u_i^e)^2}}{\sqrt{\sum_{i=1}^{n}(u_i^e)^2}} \tag{22}$$

where n is the number of collocation nodes, and u_i and u_i^e are the computed and exact solutions, respectively. The convergence rate α of the solution is estimated via $Ne(u) \simeq O(h^\alpha)$, in which h is the grid size.

Apart from the grid-refinement study, we will also investigate the effects of the MQ width on the solution accuracy.

4.1 One-dimensional problem

Consider the following fourth-order ODE

$$\frac{d^4u}{dx^4} + \frac{d^2u}{dx^2} = 16\pi^4\sin(2\pi x) - 4\pi^2\sin(2\pi x), \quad 0 \le x \le 2 \tag{23}$$

Boundary conditions are defined as $u = 0$ and $\dfrac{du}{dx} = 2\pi$ at $x = 0$ and $x = 2$.
The exact solution to this problem can be verified to be $u^e(x) = \sin(2\pi x)$.

Various grids, (7, 9,..., 71), are employed. Fig. 3 shows the accuracies of the solution and condition numbers of the system matrix against the grid size h. Results by local 5-node stencil are also included for comparison purposes. It can be seen that compact local IRBF stencils have similar values of the matrix condition number but yield much more accurate results than local IRBF stencils. The solution converges apparently as $O(h^{5.31})$ for the former and $O(h^{2.18})$ for the latter.

Fig. 4 shows a comparison of accuracy between Implementation 1 and Implementation 2, indicating that both implementations give similar levels of accuracy.

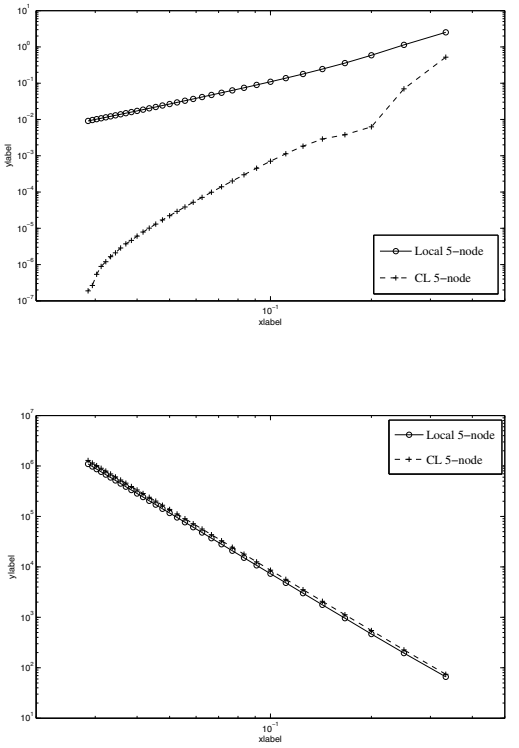

Figure 3: ODE, $\beta = 19$: solution accuracy and matrix condition number against the grid size

However, Implementation 2 yields better condition numbers than Implementation 1, probably owing to the fact that the final system matrix of the former is composed of equations derived from the PDE only.

As mentioned earlier, the value of β would have a strong influence on the solution accuracy. Since the exact solution to this problem is available, it is straightforward to obtain the optimal value of β (i.e. at which $Ne(u)$ is minimum). Table 1 shows results obtained by a fixed value and the optimal value of β for three different grids. It can be seen that using the optimal value of β significantly enhances the solution accuracy.

Several remarks can be made as follows.

(i) Inclusion of the governing equation leads to a significant improvement in not only the accuracy level but also the rate of convergence of the solution.

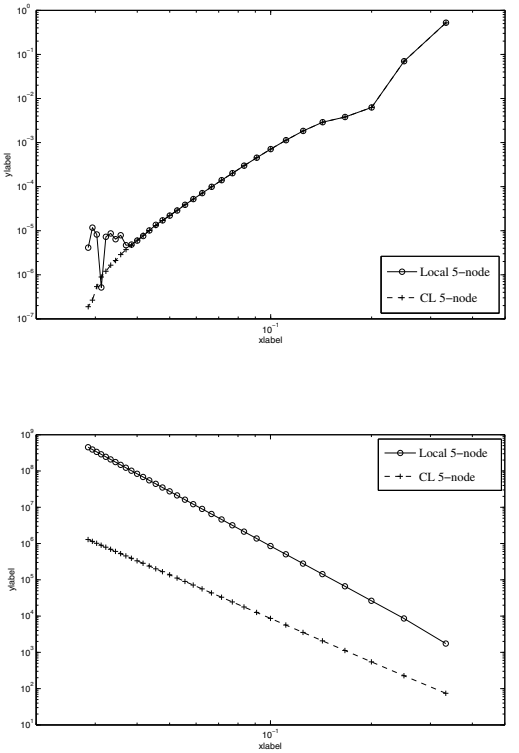

Figure 4: ODE, $\beta = 19$: solution accuracy and matrix condition number against the grid size

Table 1: ODE: Solution accuracy using a fixed value and the optimal value of β for three different grids.

h	$1/20$	$1/50$	$1/70$
	$\beta = 19$		
$Ne(u)$	7.08E-4	6.09E-6	1.89E-7
	Optimal β		
	4.3	12.9	19
$Ne(u)$	7.95E-5	1.24E-6	1.89E-7

(ii) The solution accuracy can be effectively controlled by means of the RBF width.
(iii) Implementation 2 performs better than Implementation 1.

4.2 Two-dimensional problem

Consider the biharmonic problem with the source function $f(x,y) = 16(1+\pi^4 - 2\pi^2)[\sin(2\pi x)\sinh(2y) + 16\cosh(4x)\cos(4\pi y)]$, the domain $-1/2 \le x,y \le 1/2$ and boundary conditions of Dirichlet type.

The exact solution is $u^e(x,y) = \sin(2\pi x)\sinh(2y) + \cosh(4x)\cos(4\pi y)$.

Calculations are carried out with various grids of densities $(11\times 11, 13\times 13, ..., 71\times 71)$ for both local and compact local IRBF stencils. Fig. 5 displays the solution accuracy and matrix condition number using β = 3 for various values of grid size h. The obtained results indicate that compact local 5×5-node IRBF stencils outperform local 5×5-node IRBF stencils regarding accuracy and stability (i.e. lower condition numbers). The local and compact local solutions converge as $O(h^{2.14})$ and $O(h^{4.14})$, respectively, while their matrix condition numbers grow as $O(h^{-4.0})$ and $O(h^{-3.88})$, respectively. It is also shown that the compact version works better than the standard version at fine grids.

Fig. 6 compares the solution accuracy and the matrix condition number between the two implementations of the proposed IRBF method, and Table 2 shows a comparison of the solution accuracy between the case of a fixed β value and the case of the optimal value of β. Remarks here are similar to those for 1D problems.

Table 2: PDE: Solution accuracy using a fixed value and the optimal value of β for three different grids.

h	$1/10$	$1/20$	$1/30$
	$\beta = 3$		
$Ne(u)$	3.64E-2	1.54E-3	4.86E-4
	Optimal β		
	1.32	6.86	8.52
$Ne(u)$	3.38E-2	9.21E-4	4.65E-4

5 CONCLUDING REMARKS

This paper is concerned with the development of compact local IRBF stencils for solving fourth-order ODEs and PDEs. The IRBF approximations are expressed

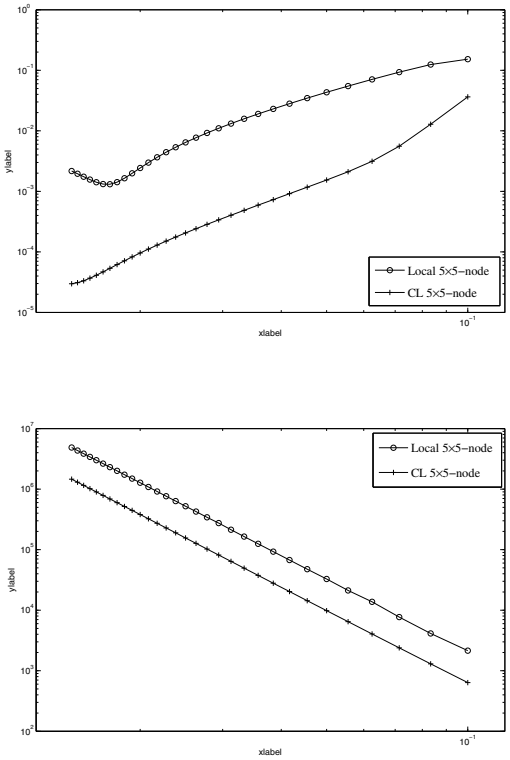

Figure 5: PDE, $\beta = 3$: accuracy and matrix condition number against the grid size

in terms of not only nodal values of the field variable but also nodal values of the ODE/PDE. The latter is incorporated through the conversion system with the help of the integration constants. The proposed stencils are successfully verified; numerical results show that high convergence rates are obtained. However, special treatments are required for the interior nodes next to the boundary. This problem is currently investigated and the outcome will be reported in our future work.

Acknowledgement The first author would like to thank CESRC, FoES and USQ for a PhD scholarship. This research was supported by the Australian Research Council.

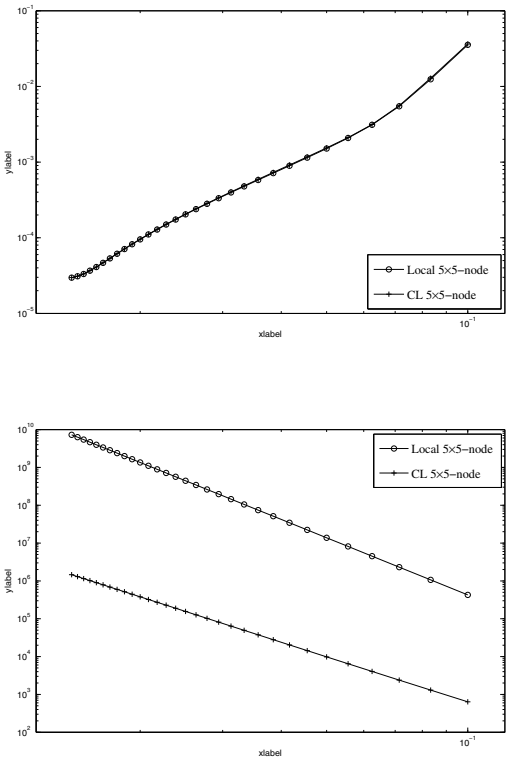

Figure 6: PDE, $\beta = 3$: Accuracy and matrix condition number against the grid size

References

An-Vo, D.-A.; Mai-Duy, N.; Tran-Cong, T. (2011): A C^2-continuous Control-Volume technique based on Cartesian grids and two-node integrated-RBF elements for second-order elliptic problems. *Computer Modeling in Engineering & Sciences*, vol. 72, pp. 299–334.

Kansa, E. (1990b): Multiquadrics - A scattered data approximation scheme with applications to computational fluid-dynamics - II Solutions to parabolic, hyperbolic and elliptic partial differential equations. *Computers & Mathematics with Applications*, vol. 19 (8-9), pp. 147–161.

Kansa, E. J. (1990a): Multiquadrics - A scattered data approximation scheme with applications to computational fluid-dynamics - I Surface approximations and partial derivative estimates. *Computers & Mathematics with Applications*, vol. 19

(8-9), pp. 127–145.

Mai-Duy, N.; Tanner, R. (2005): Computing non-Newtonian fluid flow with radial basis function networks. *International Journal for Numerical Methods in Fluids*, vol. 48(12), pp. 1309–1336.

Mai-Duy, N.; Tran-Cong, T. (2001): Numerical solution of differential equations using multiquadric radial basis function networks. *Neural Networks*, vol. 14, pp. 185–199.

Mai-Duy, N.; Tran-Cong, T. (2009): A Cartesian-grid discretisation scheme based on local integrated RBFNs for two-dimensional elliptic problems. *Computer Modeling in Engineering and Sciences*, vol. 51(3), pp. 213–238.

Mai-Duy, N.; Tran-Cong, T. (2011): Compact local integrated-RBF approximations for second-order elliptic differential problems. *Journal of Computational Physics*, vol. 230, pp. 4772–4794.

Ngo-Cong, D.; Mai-Duy, N.; Karunasena, W.; Tran-Cong, T. (2010): Free vibration analysis of laminated composite plates based on FSDT using one-dimensional IRBFN method. *Computers and Structures*, vol. 89 (1-2), pp. 1–13.